

# Post detection Integration Analysis of Adaptive Detection of Partially-Correlated $\chi^2$ Targets in The Presence of Interferers

Ben Mohamed El Mashade

Department of Electrical Engineering , Al Azhar University, Nasr City, Cairo, Egypt  
Email: ElMashade@yahoo.com

Received: January 2013

Revised: April 2013

Accepted: May 2013

## ABSTRACT

The moderately fluctuating Rayleigh and  $\chi^2$  targets represent an important class of practical targets. The illumination of this class by a coherent pulse train will return a train of correlated pulses with a correlation coefficient in the range  $0 < \rho < 1$  (intermediate between SWII and SWI models in the case of Rayleigh targets), and (intermediate between SWIV and SWIII models in the case of  $\chi^2$  targets). Therefore, it is interesting to adaptively detect this class of partially-correlated targets. On the other hand, the constant false alarm rate in the presence of variable levels of noise is usually a requirement placed on any modern radar. The CA and OS schemes are the most familiar candidates in this category of detection techniques. Our goal in this paper is to analyze their detection performances for the case where the radar receiver post-detection integrates  $M$  pulses of an exponentially correlated signal from targets which exhibit  $\chi^2$  statistics with two and four degrees of freedom. Exact formulas for the detection probabilities are derived, in the absence as well as in the presence of spurious targets. As predicted, the CA detector has the best homogeneous performance while the OS scheme gives the best target multiplicity performance when the number of outlying targets is within its allowable values.

**Keywords:** post-detection integration, partially correlated  $\chi^2$  targets, Swerling fluctuation models, CFAR detection techniques, target multiplicity environments.

## 1. Introduction

Radar's target characteristics are the driving force in the design and performance analysis of all radar systems. The target is said to be fluctuating if there is a variation in its signal's amplitude, caused by changes in target aspect angle, rotation, vibration of target scattering sources, or changes in radar wavelength. The fluctuation rate of a radar target may vary from essentially independent return amplitudes from pulse-to-pulse to significant variation only on a scan-to-scan basis. Swerling I (SWI) targets have constant amplitude over one antenna scan; however, its amplitude varies independently from scan to scan according to a  $\chi^2$  probability density function with two degrees of freedom. The amplitude of Swerling II (SWII) targets fluctuates independently from pulse to pulse according to a  $\chi^2$  probability density function with two degrees of freedom. Target fluctuation associated with a Swerling III (SWIII) model is similar to SWI, except in this case that the target power fluctuates independently from pulse to pulse according to a  $\chi^2$  probability density

function with four degrees of freedom. Finally, the fluctuation of Swerling IV (SWIV) targets is from pulse to pulse according to a  $\chi^2$  probability density function with four degrees of freedom. Swerling showed that the statistics associated with SWI and SWII models apply to targets consisting of many small scatterers of the comparable radar cross-section (RCS) values, while the statistics associated with SWIII and SWIV models apply to targets consisting of one large RCS scatterer and many small equal RCS scatterers. The advantages of the Swerling target models are that they bracket a large number of real target classes [1-6]. However, recent investigations of the target cross section fluctuation statistics indicate that some targets may have probability of the detection curves which lie considerably outside the range of cases which are satisfactorily bracketed by the Swerling cases. An important class of targets is represented by the so-called moderately fluctuating Rayleigh and  $\chi^2$  targets [7], when illuminated by a coherent pulse train, return a train of correlated pulses with a correlation coefficient

in the range  $0 < \rho < 1$ . The detection of this type of fluctuating targets is therefore of the great interest.

Generally, target fluctuation lowers the probability of the detection, or equivalently reduces the SNR. Pulse integration improves SNR and correspondingly the detection probability, but the amount of improvement depends upon the method of integration, which may be accomplished in either the IF section prior the square-law device or in the video section after the square-law device of the radar receiver. There is a considerable difference between the two types of integration. Integration before the device is defined as coherent or Pre-detection integration, while the second type is known as Non-coherent or Post-detection integration. Coherent integration requires the phase of the echo signal to be preserved during the summing process; that is the phase of the received signal must remain constant with respect to the phase of a known sinusoid. Thus, all Doppler information about the target and Doppler information introduced by the relative target and radar motion into the signal must also be preserved. On the other hand, the Non-coherent integration is the most common type of integration used in the radar systems. If  $M$  pulses were integrated non-coherently, the final SNR would be less than that for coherent integration, which is less than  $M$  times that of a single pulse. The relative increase in the noise energy is caused by the rectifying characteristic of the square-law detector, which prevents some of the noise self cancellation that would otherwise occur. The integration efficiency of a post-detection integrator is thus always less than that of a Pre-detection integrator. Furthermore, Non-coherent integration cannot preserve information such as Doppler data that is already lost. However, the ease of implementing a Post-detection pulse integrator usually outweighs any advantages achieved by the improvement of the integration efficiency that would be obtained by the use of a Pre-detection pulse integrator. Post-detection pulse integration, therefore, is usually implemented although not ideally preferred. Non-coherent integration can be applied to all four Swerling models; however, Coherent integration cannot be used when the target fluctuation is either SWII or SWIV, because the target amplitude de-correlates from pulse to pulse (fast fluctuation) for SWII and SWIV models, and thus phase coherency cannot be maintained.

Many radar systems operate in an environment where the noise generated within its own receiver is not the dominant source of interference. Undesired echoes from rain, clutter, and unwanted signals from other radiating sources often exceed the receiver noise level. These sources of interference may completely obliterate the radar display, or they may overload a computer that is making Yes/No decisions as to which echoes are valid targets of interest. To reduce this problem, radar

detection processing can use an algorithm to estimate the clutter energy in the target test cell and then adjust the detection threshold to reflect changes in this energy at the different test cell positions. The threshold algorithms use the detection cells near the target test cell to estimate the background clutter level, and then set the threshold to guarantee the desired false alarm probability. This technique approaches a constant false alarm rate (CFAR) in most clutter backgrounds. The CFAR system uses the fact that the amplitude variation of the weather and sea clutter has a Rayleigh distribution, and is capable of reducing the clutter output to about the same level as the receiver noise level. As a consequence, much attention has been paid to the task of designing and assessing these adaptive detection techniques. The CA- and OS-CFAR detectors are the most widely used ones in the CFAR world [8-11]. While the performance of the CA detector is optimum in homogeneous situations, this performance degrades rapidly in non-ideal conditions caused by multiple target and non-uniform clutter. The OS processor, on the other hand, is a CFAR technique, which is relatively immune to non-homogeneous cases caused by outlying targets and clutter edges. This technique relies on ordering the samples in the reference window and takes an appropriate reference cell to estimate the clutter power level. The OS trades a small loss in detection performance, relative to the CA, in the ideal conditions for much less performance degradation in the non-ideal conditions.

From this brief discussion, it is obvious that there is a need of considering the performance of various CFAR algorithms, which coherently process received signals that are multi-dimensional in nature. In the CFAR context, the results of such analysis may be useful in assessing the potential benefits of utilizing the capability of radar systems that can acquire and process multi-dimensional (or vector) signals. Our goal in the present paper is to analyze the performance of CA- and OS-CFAR detectors for partially-correlated  $\chi^2$  targets with two and four degrees of freedom in the absence as well as in the presence of the spurious targets. In section II, we formulate the problem and compute the characteristic function of the post-detection integrator output for the case where the signal fluctuation obeys  $\chi^2$  statistics with two and four degrees of freedom. The performance of the schemes under the consideration is analyzed, in the ideal (homogeneous) background environment, in section III. Section IV deals with the problem of multiple-target environment and the performance evaluation of the CA and OS detectors in these situations. In section V, we present a brief discussion along with our conclusions.

## 2. Statistical Model Description

Let the input target signal and noise to the square-law detector are represented by the complex vectors  $u + jv$  and  $a + jb$ , respectively.  $u$  and  $v$  represent the in-phase and quadrature components of the target signal at the square-law detector,  $a$  and  $b$  represent the in-phase and quadrature components of the noise, respectively. The target is assumed to be independent of the noise and the in-phase samples are assumed to be independent and identically distributed (IID) with the Gaussian probability density function (PDF), while the target samples are assumed to be identically distributed but correlated. The output of  $M$ -pulse non-coherent integrator, normalized to the noise power, is

$$v \triangleq \frac{1}{2\psi} \sum_{\ell=1}^M (|u_{\ell} + a_{\ell}|^2 + |v_{\ell} + b_{\ell}|^2) \quad (1)$$

Let the in-phase received target signal and noise vectors be  $U$  and  $A$ , respectively, where

$$U \triangleq [u_1, u_2, u_3, \dots, u_M]^T \quad \text{and} \quad A \triangleq [a_1, a_2, a_3, \dots, a_M]^T \quad (2)$$

The characteristic function (CF) of  $v$  can be expressed as

$$C_v(\omega) \triangleq \int_{-\infty}^{\infty} p_v(y) \exp(-\omega y) dy \\ = \left\{ \int_{-\infty}^{\infty} \int_{-\infty}^{\infty} p_U(u) p_A(a) \exp\left(-\frac{\omega}{2\psi} \sum_{i=1}^M |u_i + a_i|^2\right) da du \right\}^2 \quad (3)$$

In the above expression,  $p_U(u)$  and  $p_A(a)$  denote the joint probability density functions (PDF's) of  $U$  and  $A$ , respectively. From our previous assumptions, one can write the joint PDF of  $A$  as

$$p_A(a) = \frac{1}{(2\pi\psi)^{M/2}} \exp\left(-\frac{1}{2\psi} \sum_{j=1}^M a_j^2\right) \quad (4)$$

The substitution of Eq.(4) in Eq.(3) yields

$$C_v(\omega) = \left\{ \left(\frac{1}{2\pi\psi}\right)^{M/2} \int_{-\infty}^{\infty} p_U(u) du \int_{-\infty}^{\infty} \exp\left[-\frac{1}{2\psi} \sum_{i=1}^M (\omega |u_i + a_i|^2 + |a_i|^2)\right] da \right\}^2 \\ = \frac{1}{(\omega+1)^M} \left\{ \int_{-\infty}^{\infty} p_U(u) \exp\left(-\frac{\omega}{2\psi(\omega+1)} \sum_{j=1}^M |u_j|^2\right) du \right\}^2 \quad (5)$$

A radar target whose return varies up and down in amplitude as a function of time is known as a fluctuating target. The fluctuation rate may vary from essentially independent return amplitudes from pulse-to-pulse to significant variation only on a scan-to-scan basis. Because the exact nature of the change is difficult to predict, a statistical description is often adopted to characterize the target radar cross section. There are many probability density functions for target cross section which are used to characterize fluctuating targets. The more important PDF is the so-called  $\chi^2$  distribution with  $2\kappa$  degrees of freedom. This  $\chi^2$  model approximates a target with a large reflector and a group of small reflectors, as well as a large reflector over a small range of aspect values. The  $\chi^2$  family includes the Rayleigh (Swerling cases I & II) model, the four-degree of freedom model (Swerling models III & IV), the

Weinstock model ( $\kappa < 1$ ) and the generalized model ( $\kappa$  a positive real number). The  $\chi^2$  models are used to represent complex targets such as aircraft and have the characteristic that the distribution is more concentrated about the mean as the value of the parameter  $\kappa$  is increased. The SWI and SWIII models represent scan-to-scan fluctuating targets, while the SWII and SWIV cases represent fast pulse-to-pulse fluctuating targets. The  $\chi^2$ -distribution with  $2\kappa$  degrees of freedom is given by

$$p\left(\frac{\sigma}{\bar{\sigma}}\right) = \frac{1}{\Gamma(\kappa)} \left(\frac{\kappa}{\sigma}\right)^{\kappa} \sigma^{\kappa-1} \exp\left(-\frac{\kappa}{\sigma}\right) U(\sigma) \quad (6)$$

$\bar{\sigma}$  represents the average cross section over all target fluctuations and  $U(\cdot)$  denotes unit step function. When  $\kappa=1$ , the PDF of Eq.(6) reduces to the exponential or Rayleigh power distribution that applies to the Swerling case I. Swerling cases II, III, and IV correspond to  $\kappa=M$ , 2, and  $2M$ , respectively. When  $\kappa$  tends to infinity, the  $\chi^2$ -distribution corresponds to the non-fluctuating target. It is finally of important to note that the  $\chi^2$ -distribution with  $2\kappa$  degrees of freedom can be obtained by adding squared magnitude of  $\kappa$  complex Gaussian random variables.

### 2.1. $\chi^2$ -Distribtion with two-degrees of freedom

If  $\kappa=1$ , then  $\sigma$  may be generated as  $\sigma=w_1^2+w_2^2$ , where  $w_i$ 's are independent and identically distributed (IID) Gaussian random variables, each with zero mean and  $\bar{\sigma}/2$  variance. The magnitude of the in-phase component  $u$  ( $u=|w_1|$ ) has a PDF given by

$$p_v(u) du = p_{w_1}(w_1) dw_1 = \frac{1}{\sqrt{2\pi\alpha}} \exp\left(-\frac{w_1^2}{2\alpha}\right) dw_1 \quad \text{with} \quad \alpha \triangleq \frac{\bar{\sigma}}{2} \quad (7)$$

To accommodate an  $M \times 1$  vector of correlated chi-square RV's with two degrees of freedom, we introduce the PDF of the  $M$ -dimensional vector  $W_1$ . Therefore, the joint PDF of  $u_i$ 's,  $i=1, 2, \dots, M$ , has a form given by

$$p_v(u) du = p_{w_1}(w_1) dw_1 = \left(\frac{1}{2\pi\alpha}\right)^{M/2} \frac{1}{|\Lambda|^{M/2}} \exp\left(-\frac{w_1^T \Lambda^{-1} w_1}{2\alpha}\right) dw_1 \quad (8)$$

$\Lambda$  is the correlation matrix of  $u_1, u_2, \dots, u_M$  and  $T$  denotes transposition. With  $I$  denoting the identity matrix, the substitution of Eq.(8) into Eq.(5) yields

$$C_v(\omega) = \frac{1}{(\omega+1)^M} \left\{ \int_{-\infty}^{\infty} \frac{1}{(2\pi\alpha)^{M/2} \sqrt{|\Lambda|}} \exp\left[-\frac{1}{2\alpha} \left(w_1^T \Lambda^{-1} w_1 + \frac{\alpha}{\psi} \omega w_1\right)\right] dw_1 \right\}^2 \quad (9)$$

If we let the average signal-to-noise ratio (SNR)  $\alpha/\psi=\Omega$ , Eq.(9) can be re-expressed as

$$C_v(\omega) = \prod_{\ell=1}^M \frac{1}{1 + (1 + \lambda_{\ell} \Omega) \omega} \quad (10)$$

$\lambda_i$ 's are the non-negative eigenvalues of  $\Lambda$ . The CF of Eq.(10) for the SWI target fluctuation model is represented by choosing  $\lambda_1=M$ ,  $\lambda_i$ 's=0,  $i=2, 3, \dots, M$ ,

and that for the SWII case can be modeled by letting  $\lambda_i's=1, i=1, 2, \dots, M$ . For the CFAR processor performance analysis to be simple, the above equation can be put in another clarified form as

$$C_v(\omega) = \prod_{j=1}^M \frac{d_j}{\omega + d_j} \quad \text{with} \quad d_j \triangleq \frac{1}{1 + \Omega \lambda_j} \quad (11)$$

**2.2.  $\chi^2$ -Distribution with four-degrees of freedom**

If  $\kappa=2$ , then  $\sigma$  and the squared magnitude of its in-phase component,  $u$ , may be generated as follows:

Let  $w_i's, i=1, \dots, 4$ , be IID Gaussian random variables, each one is of zero mean and of  $\alpha = \sigma^2/4$  variance,  $\sigma$  and  $|u|$  are given by

$$\sigma = \sqrt{w_1^2 + w_2^2 + w_3^2 + w_4^2} \quad \text{and} \quad |u| \triangleq \sqrt{w_1^2 + w_2^2} \quad (12)$$

Since  $w_1$  and  $w_2$  are IID, one may write

$$p_u(u) du = p_{w_1}(w_1) p_{w_2}(w_2) dw_1 dw_2 = \frac{1}{2\pi\alpha} \exp\left[-\frac{w_1^2 + w_2^2}{2\alpha}\right] dw_1 dw_2 \quad (13)$$

Therefore, the joint PDF of  $u_1, u_2, \dots, u_M$  is of the form

$$p_U(u) du = p_{w_1}(w_1) p_{w_2}(w_2) dw_1 dw_2 = \left(\frac{1}{2\pi\alpha}\right)^M \left(\frac{1}{|\Lambda|}\right) \exp\left[-\frac{w_1^T \Lambda^{-1} w_1 + w_2^T \Lambda^{-1} w_2}{2\alpha}\right] dw_1 dw_2 \quad (14)$$

Where  $\Lambda$  is the correlation matrix of  $w_1$  and  $w_2$ . Note that  $w_1$  and  $w_2$  are uncorrelated, but components of  $w_1$  are correlated with each other, as the components of  $w_2$ . Therefore, Eq. (5) can be rewritten as

$$C_v(\omega) = \left(\frac{1}{\omega+1}\right)^M \left\{ \int_{-\infty}^{\infty} \left(\frac{1}{2\pi\alpha}\right)^M \frac{1}{|\Lambda|} \exp\left[-\frac{1}{2\alpha} \left\{ w_1^T \left( \Lambda^{-1} + \frac{\alpha}{\psi} \frac{\omega}{\omega+1} I \right) w_1 \right\} \right] * \left\{ \exp\left[-\frac{1}{2\alpha} \left\{ w_2^T \left( \Lambda^{-1} + \frac{\alpha}{\psi} \frac{\omega}{\omega+1} I \right) w_2 \right\} \right] dw_1 dw_2 \right\} \right\} \quad (15)$$

If we let the average SNR ( $2\alpha/\psi$ ) as  $\Omega$ , the above equation can be re-expressed as

$$C_v(\omega) = \prod_{\ell=1}^M \frac{\omega + 1}{\left\{ \left( 1 + \Omega \frac{\lambda_\ell}{2} \right) \omega + 1 \right\}^2} \quad (16)$$

The CF of Eq.(16) for the Swerling III target fluctuation model is represented by choosing  $\lambda_1=M, \lambda_i's=0, i=2, 3, \dots, M$ , and that for the Swerling IV case can be modeled by letting  $\lambda_i's=1, i=1, 2, \dots, M$ . To simplify the detection performance evaluation of the CFAR processors, the above equation can be reformatted to have an easily mathematical form such as

$$C_v(\omega) = \prod_{j=1}^M (\omega+1) \left\{ \frac{b_j}{\omega + b_j} \right\}^2 \quad \text{with} \quad b_j \triangleq \frac{1}{1 + \Omega \lambda_j/2} \quad (17)$$

In view of Eqs.(11 & 17), the solution for partially-correlated case requires the computation of the eigenvalues of the correlation matrix  $\Lambda$ . It is assumed here that i) the statistics of the signal are stationary, and ii) the signal can be represented by a first order Markov process. Under these assumptions,  $\Lambda$  is a Toeplitz nonnegative definite matrix . Thus,

$$\Lambda = \begin{bmatrix} 1 & \rho & \rho^2 & \dots & \rho^{M-2} & \rho^{M-1} \\ \rho & 1 & \rho & \dots & \rho^{M-3} & \rho^{M-2} \\ \rho^2 & \rho & 1 & \dots & \rho^{M-4} & \rho^{M-3} \\ \vdots & \vdots & \vdots & \ddots & \vdots & \vdots \\ \rho^{M-2} & \rho^{M-3} & \rho^{M-4} & \dots & 1 & \rho \\ \rho^{M-1} & \rho^{M-2} & \rho^{M-3} & \dots & \rho & 1 \end{bmatrix} \quad 0 \leq \rho \leq 1 \quad (18)$$

Eqs.(11, 17 &18) are the basic formulas of our analysis in this manuscript.

The PDF of the output of the  $i$ th test tap is given by the Laplace inverse of Eq. (11), in the case of  $\chi^2$  distribution with two degrees of freedom, or Eq.(17), in the case of  $\chi^2$  fluctuation with four degrees of freedom, after making some minor modifications. If the  $i$ th test tap contains noise alone, we let  $\Omega=0$ , that is the average noise power at the receiver input is  $\psi$ . If the  $i$ th range cell contains a return from the primary target, it rests as it is without any modifications, where  $\Omega$  represents the strength of the target return at the receiver input. On the other hand, if the  $i$ th test cell is corrupted by interfering target return,  $\Omega$  must be replaced by I, where I denotes the interference-to-noise (INR) at the receiver input.

The essence of CFAR is to compare the decision statistic  $v$  with an adaptive threshold TZ, see Fig.(1).

The threshold coefficient T is a constant scale factor used to achieve a desired false alarm rate for a given window size N when the background noise is homogeneous. The statistic Z is a random variable) whose distribution depends upon the particular CFAR chosen scheme and the underlying distribution of each of the reference range samples. Since the unknown noise power level estimate Z is a random variable, the processor performance is determined by calculating the average values of the false alarm and detection probabilities.

The detection probability of a CFAR processor for  $\chi^2$  targets with two degrees of freedom can be obtained by substituting Eq.(11) into the definition of  $P_d$ , which gives

$$P_d = - \sum_j \text{res} \left\{ \prod_{i=1}^M \frac{d_i}{\theta + d_i} \frac{C_z(-T\theta)}{\theta}, \theta_j \right\} = \sum_{j=1}^M \prod_{i=1, i \neq j}^M \frac{d_i}{d_i - d_j} C_z(T d_j) \quad (19)$$

In the above expression, *res* stands for the residue.

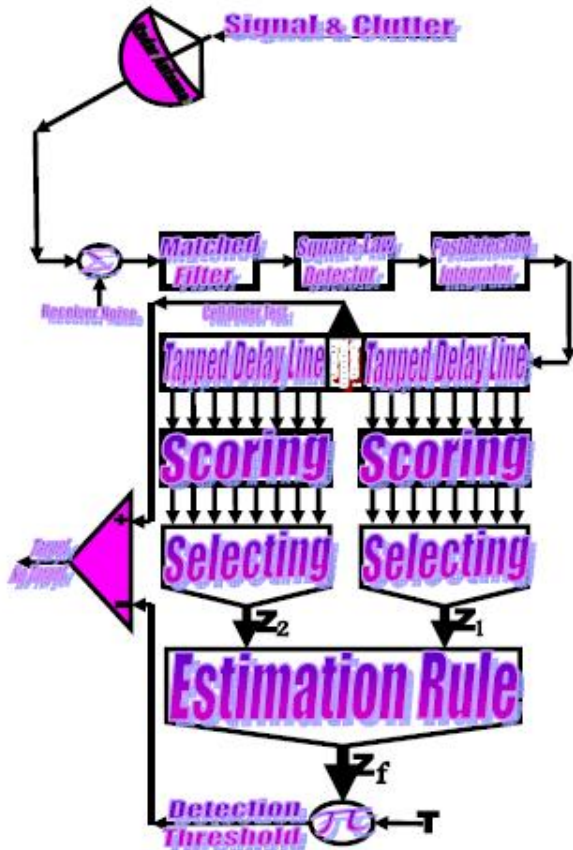


Fig1. Block diagram of adaption detector using M-pulse non-coherent integration

On the other hand, when the fluctuation of the primary target follows the  $\chi^2$  distribution with four degrees of freedom,  $C_v(\omega)$  takes the following simplified form

$$C_v(\omega) = \prod_{j=1}^M b_j^2 \frac{\omega + 1}{(\omega + b_j)^2} = \sum_{j=1}^M \left\{ \frac{g_j}{\omega + b_j} + \frac{h_j}{(\omega + b_j)^2} \right\} \quad (20)$$

Where

$$h_j \triangleq b_j^2 (1 - b_j) \prod_{\substack{k=1 \\ k \neq j}}^M b_k^2 \frac{1 - b_j}{(b_k - b_j)^2} \quad (21)$$

And

$$g_j \triangleq h_j \left\{ \frac{M}{1 - b_j} - 2 \sum_{\substack{l=1 \\ l \neq j}}^M \frac{1}{b_l - b_j} \right\} \quad (22)$$

The substitution of Eq.(25) into the definition of the detection probability gives the processor detection performance for  $\chi^2$  targets with four degrees of freedom, which becomes

$$P_d = \sum_{j=1}^M \left\{ \frac{g_j}{b_j} C_z(r b_j) + \frac{h_j}{b_j} \left[ \frac{C_z(r b_j)}{b_j} + \frac{d}{d\omega} \left| C_z(-T\omega) \right|_{\omega=-b_j} \right] \right\} \quad (23)$$

To obtain the relationship between the false alarm probability  $P_{fa}$  and the thresholding constant T, it is assumed that no target is present in the test cell ( $A=0$ ).

Therefore, as M-pulse non-coherent integration is used,  $P_{fa}$  can be calculated as

$$P_{fa} = - \frac{1}{\Gamma(M)} \frac{d^{M-1}}{d\omega^{M-1}} \left\{ \frac{C_z(-T\omega)}{\omega} \right\} \Big|_{\omega=-1} \quad (24)$$

In this case,  $C_v(\omega)$  has an Mth order pole at  $\omega=-1$ . Thus,

$$P_{fa} = \sum_{j=0}^{M-1} \frac{1}{\Gamma(j+1)} \frac{d^j}{d\omega^j} \left\{ C_z(-T\omega) \right\} \Big|_{\omega=-1} \quad (25)$$

It is important to note that the above expression for the rate of false alarm is verified either for  $\chi^2$  targets with two degrees of freedom or for  $\chi^2$  targets with four degrees of freedom. Moreover, the characteristic function of the noise power level estimate 'Z' is the backbone of the processor performance analysis, as shown in Eqs.(24, 28 & 30), either in homogeneous or non-homogeneous background environments. Therefore, our scope in the following subsections is to calculate this important quantity for the two processors under consideration

### 3. Non-homogeneous Performance Analysis of CFAR Schemes

The performance of the CFAR algorithms for uniform clutter model can be considered as special case of their behavior against non-homogeneous environments. Therefore, the non-homogeneous analysis of CFAR detection of the fluctuating targets is more general than the homogeneous situation and consequently it deserves to be tackled. In the world of CFAR detection of the radar targets, there are two basic problems associated with non-homogeneous treatment of the processor performance: clutter edges and multiple-target situations. Clutter edges, on the other hand, are used to describe transition areas between regions with very different noise characteristics. Since we are concerned here with partially correlated  $\chi^2$  targets, this situation is of secondary scope. On the other hand, multiple target situations occur occasionally in radar signal processing when two or more targets are at a very similar range. The consequent masking of one target by the others is called suppression. These interferers can arise from either real object returns or pulsed noise jamming. From a statistical point of view, this implies that the reference samples, although still independent of one another, are no longer identically distributed. Let us now examine the dependence of the performance of the CFAR procedures on the accurate knowledge of the target fluctuation model when the reference window is contaminated with a fluctuating interfering target returns. In our study of the non-homogeneous background, the amplitudes of all the targets present amongst the candidates of the reference window are assumed to be of the same strength and to fluctuate in accordance with the partially-correlated  $\chi^2$

fluctuation model with correlation coefficient  $\rho_i$ . The interference-to-noise ratio (INR) for each of the spurious targets is taken as a common parameter and is denoted by I.

**a. Cell-Averaging (CA) Detector**

A simple approach to achieve the CFAR condition is to set the detection threshold on the basis of the average noise power in a given number of reference cells where each of them is assumed to contain no target. Such a scheme is denoted as cell-averaging (CA) CFAR processor. This detector is specifically tailored to provide good estimates of the noise power in the exponential PDF. In this CFAR detection technique, the total noise power level is estimated by the sum of N range cells of the reference window. Under the assumption that the surrounding range cells contain independent Gaussian noise samples with the same variance, this sum of the reference cells represents the maximum likelihood estimate of the common variance. This is a complete, sufficient statistic for the noise power  $\psi$  under the assumption of exponentially distributed homogeneous background.

To analyze the CA performance when the reference window no longer contains radar returns from a homogeneous background, the assumption of statistical independence of the reference cells is retained. Suppose that the reference window contains r cells from interfering target returns with background power of  $\psi(1+I)$  and N-r cells from clear background with noise power  $\psi$ . Thus, the estimated total noise power level is obtained from

$$Z_{ca} \triangleq \sum_{j=1}^r q_{ij} + \sum_{k=r+1}^M \sum_{l=1}^r q_{kl} \triangleq \sum_{i=1}^r X_i + \sum_{k=1}^{N-r} Y_k \triangleq X + Y \quad (26)$$

If the reference sample contains no target return; i.e. its content is pure clear background return, it has a CF of the same form as that of v with the exception that  $\Omega$  must be set to zero. Therefore, eliminating  $\Omega$  in either Eq.(11) or Eq.(17) leads to

$$C_{Y_k}(\omega) = \left( \frac{1}{\omega + 1} \right)^M \quad (27)$$

Since the random variables  $Y_i$ 's are assumed to be statistically independent and identically distributed, the vector Y of dimension N-r has a CF given by

$$C_Y(\omega) = \left( \frac{1}{\omega + 1} \right)^M \quad (28)$$

On the other hand, the random variable representing the interfering target return 'X' has a CF of the same form as that given by Eq.(11), when the extraneous targets fluctuate in accordance with  $\chi^2$  model with two-degrees of freedom, and as that given by Eq.(16), in the case where the fluctuation of the spurious targets follows  $\chi^2$  model with four-degrees of freedom. In both

cases, A (SNR of the primary target) should be replaced by I (INR of the secondary target). Thus,

$$C_X(\omega) = \begin{cases} \prod_{i=1}^M \frac{f_i}{\omega + f_i} & \& f_i \triangleq \frac{1}{1 + I \lambda_i} \quad \text{for } \chi^2 \text{ with 2 degrees of Freedom} \\ \prod_{j=1}^M (\omega + 1) \left( \frac{e_j}{\omega + e_j} \right)^2 & \& e_j \triangleq \frac{1}{1 + 1/2 \lambda_j} \quad \text{for } \chi^2 \text{ with 4 degrees of Freedom} \end{cases} \quad (29)$$

In the above expression,  $\lambda_i$ 's represent the nonnegative eigenvalues of the correlation matrix, with  $\rho = \rho_i$  in Eq.(18), associated with the spurious target returns. Since the elements of the vector X are assumed to be statistically independent, its CF takes the form:

$$C_X(\omega) = \begin{cases} \left[ \prod_{i=1}^M \frac{f_i}{\omega + f_i} \right]^r & \chi^2 \text{ with 2 degrees of Freedom} \\ \left[ \prod_{j=1}^M (\omega + 1) \left( \frac{e_j}{\omega + e_j} \right)^2 \right]^r & \text{for } \chi^2 \text{ with 4 degrees of Freedom} \end{cases} \quad (30)$$

Since the vectors X and Y of Eq.(31) are jointly independent, the CF of the RV  $Z_{ca}$  is simply given by the product of their CF's. Therefore, the noise level estimate of the CA processor, operating in multi target environment, has a simple CF of the form:

$$C_{Z_{ca}}(\omega) = C_X(\omega) C_Y(\omega) \quad (31)$$

On the other hand, the derivative of the CF of the test statistic of the CA procedure, when the interfering targets fluctuate in accordance with  $\chi^2$  model of four degrees of freedom, can be easily computed as

$$\frac{d}{d\omega} C_{Z_{ca}}(\omega) = \left\{ \prod_{k=1}^M e_k^2 \frac{\omega + 1}{(\omega + e_k)^2} \right\}^r \left\{ \frac{1}{\omega + 1} \right\}^{M(N-r)} \left\{ \frac{M(2r-N)}{\omega + 1} - 2 \sum_{i=1}^M \frac{r}{\omega + e_i} \right\} \quad (32)$$

It is of importance to note that the homogeneous evaluation of the processor performance can be treated as a special case of its behavior against multi-target situation by making the background environment free of any spurious targets ( $r=0$ ). In other words, when the CA-CFAR scheme processing data from uniform clutter, its estimate of the noise power level has a CF given by:

$$C_{Z_{ca}}(\omega) = (\omega + 1)^{-MN} \quad (33)$$

Once the CF of the noise power level estimate is obtained, the detector performance evaluation is completely determined either the primary target fluctuates in accordance with  $\chi^2$  model with two or its fluctuation follows  $\chi^2$  statistics with four degrees of freedom as we have previously demonstrated, where

$$\frac{d^k}{d\omega^k} C_{Z_{ca}}(\omega) = (-\alpha)^k (L)_k (\alpha \omega + 1)^{-(L+k)} \quad \& \quad L \triangleq MN \quad (34)$$

The Pochhammer symbol  $(x)_k$  is as defined in [12]:

$$(x)_k \triangleq \frac{\Gamma(x)}{\Gamma(x+k)} = \begin{cases} 1 & \text{for } k=0 \\ x(x+1)(x+2)\dots(x+k-1) & \text{for } k=1,2,3,\dots \end{cases} \quad (35)$$

The rationale for the CA type of CFAR schemes is that by choosing the mean, the optimum CFAR processor in a homogeneous background when the

reference cells contain IID observations governed by exponential distribution is achieved. As the size of the reference window increases, the detection probability approaches that of the optimum detector which is of the fixed threshold architecture [13].

We repeat again that once CF of the noise power level,  $Z_{CA}$ , is obtained, the processor performance evaluation is completely determined, in the case where the fluctuation of the spurious targets follows the  $\chi^2$  model with either two or four degrees of freedom, as we have previously demonstrated.

**b. Ordered-Statistics (OS) Detector**

The performance of CA-CFAR detector degrades rapidly in non-ideal conditions caused by multi targets and non-uniform clutter. The ordered-statistic (OS) CFAR is an alternative to the CA processor. The OS trades a small loss in the detection performance, relative to the CA scheme, in the ideal conditions for much less performance degradation in the non-homogeneous background environments.

Order statistics characterize amplitude information by ranking observations in which differently ranked outputs can estimate different statistical properties of the distribution from which they stem. The order statistic corresponding to a rank K is found by taking the set of N observations  $Q_1, Q_2, \dots, Q_N$  and ordering them with respect to increasing magnitude in such a way that

$$Q_{(1)} \leq Q_{(2)} \leq \dots \leq Q_{(K-1)} \leq Q_{(K)} \leq Q_{(K+1)} \leq \dots \leq Q_{(N)} \tag{36}$$

Where  $Q_{(K)}$  is the Kth order statistic. The central idea of the OS-CFAR procedure is to select one certain value from the above sequence and to use it as an estimate Z for the average clutter power as observed in the reference window. Thus,

$$Z_{os} = Q_{(K)} \quad , \quad K \in \{1, 2, 3, \dots, N\} \tag{37}$$

We will denote by OS(K) the OS scheme with parameter K. The value of K is generally chosen in such a way that the detection of radar target in the homogeneous background environment is maximized.

In order to analyze the processor performance when there are interfering target returns amongst the contents of the reference window, the assumption of statistical independence of the reference cells is retained. Consider the situation where there are r reference samples contaminated by extraneous target returns, each with power level  $\psi(1+I)$ , and the remaining N-r reference cells contain thermal noise only with power level  $\psi$ . Under these assumptions, the Kth ordered sample, which represents the noise power level estimate in the OS detector, has a cumulative distribution function (CDF) given by [14]:

$$F_{Z_{os}}(z) = \sum_{i=K}^N \sum_{j=\max(0, i-r)}^{\min(i, N-r)} \binom{N-r}{j} \binom{r}{i-j} [1 - F_c(z)]^{N-r-j} \{F_c(z)\}^j [1 - F_s(z)]^{-i+j} \{F_s(z)\}^{i-j} \tag{38}$$

In the above expression,  $F_c(z)$  represents the CDF of the cell that contains clutter background whilst  $F_s(z)$  denotes the same thing for the cell that has spurious target return.

In order to calculate the above formula, first these two important characteristics must be computed. For clear background, the CDF of its cell has a Laplace transformation similar to that given by Eq.(32) after dividing it by  $\omega$ . Thus, this CDF can be obtained by taking the Laplace inverse of the resulting version which gives:

$$F_c(x) = L^{-1} \left\{ \frac{1}{\omega(\omega+1)^M} \right\} = 1 - \sum_{i=0}^{M-1} \frac{z^i}{\Gamma(i+1)} e^{-z} U(z) \tag{39}$$

$L^{-1}$  represents the Laplace inverse operator and  $U(\cdot)$  denotes the nit-step function.

The CDF of the reference cell that contains a spurious target return, when this target fluctuates in accordance with  $\chi^2$  with two degrees of freedom, can be calculated from:

$$F_s(z) = L^{-1} \left\{ \frac{1}{\omega} \prod_{\ell=1}^M \frac{1}{1+(1+I\lambda_\ell)\omega} \right\} = 1 - \sum_{\ell=1}^M \zeta_\ell e^{-\zeta_\ell z} \tag{40}$$

with

$$\zeta_\ell \triangleq \prod_{k=1}^M \frac{1+I\lambda_k}{I(\lambda_k - \lambda_\ell)} \quad \& \quad c_\ell \triangleq \frac{1}{1+I\lambda_\ell} \tag{41}$$

On the other hand, if the interfering target's fluctuation follows  $\chi^2$  model with four degrees of freedom,  $F_s(z)$  takes the form

$$F_s(z) = L^{-1} \left\{ \frac{1}{\omega} \prod_{j=1}^M \frac{\varepsilon_j^2 (\omega+1)}{(\omega+\varepsilon_j)^2} \right\} = 1 - \sum_{j=1}^M (a_j + z t_j) \exp(-\varepsilon_j z) \tag{42}$$

With

$$a_j \triangleq \varepsilon_j (1 - \varepsilon_j) \prod_{\substack{i=1 \\ i \neq j}}^M \left( \frac{\varepsilon_i}{\varepsilon_i - \varepsilon_j} \right)^2 \left\{ \frac{M}{1 - \varepsilon_j} + \frac{1}{\varepsilon_j} - \sum_{\substack{\ell=1 \\ \ell \neq j}}^M \frac{2}{\varepsilon_\ell - \varepsilon_j} \right\} \tag{43}$$

And

$$t_j \triangleq \varepsilon_j (1 - \varepsilon_j) \prod_{\substack{k=1 \\ k \neq j}}^M \frac{\varepsilon_k^2 (1 - \varepsilon_j)}{(\varepsilon_k - \varepsilon_j)^2} \quad \& \quad \varepsilon_j \triangleq \left( 1 + I \frac{\lambda_j}{2} \right)^{-1} \tag{44}$$

Since  $F(x)=1-[1-F(x)]$ , Eq.(38) can be written in another simpler form as [15]:

$$F_{Z_{os}}(z) = \sum_{i=K}^N \sum_{j=\max(0, i-r)}^{\min(i, N-r)} \binom{N-r}{j} \binom{r}{i-j} \sum_{k=0}^j \binom{j}{k} (-1)^{j-k} [1 - F_c(z)]^{N-r-k} \sum_{\ell=0}^{i-j-k} \binom{i-j-k}{\ell} (-1)^{i-j-\ell} [1 - F_s(z)]^{i-k-\ell} \tag{45}$$

By substituting Eq.(39) along with Eq.(45), into Eq.(49) one obtains, for  $\chi^2$  target fluctuation with two degrees of freedom,

$$F_{Z_{os}}(z) = \sum_{i=K}^N \sum_{j=\max(0, i-r)}^{\min(i, N-r)} \binom{N-r}{j} \binom{r}{i-j} \sum_{k=0}^j \sum_{\ell=0}^{i-j-k} \binom{j}{k} \binom{i-j-k}{\ell} (-1)^{i-k-\ell} \left\{ \sum_{m=0}^{M-1} \frac{z^m}{\Gamma(m+1)} \exp(-z) \right\}^{N-r-k} * \left\{ \sum_{n=1}^M \zeta_n \exp(-\zeta_n z) \right\}^{i-k-\ell} \tag{46}$$

On the other hand, if the extraneous targets fluctuate according to  $\chi^2$  model with four degrees of freedom, Eq.(45) takes a modified version of the form:

$$F_{Z_{OS}}(z) = \sum_{i=k}^N \sum_{j=\max(\theta, i-r)}^{\min(\theta, N-r)} \binom{N-r}{j} \binom{r}{i-j} (-1)^{i-k-\ell} \left\{ \sum_{m=0}^{M-1} \frac{z^m}{\Gamma(m+1)} \exp(-z) \right\}^{N-r-i} * \left\{ \sum_{n=1}^M (a_n + z t_n) \exp(-\theta_n z) \right\}^{r-\ell} \quad (47)$$

To determine the detection performance of the OS-CFAR processor, it is important to calculate the Laplace transform for its test statistic, where the false alarm and detection probabilities are completely dependent on this transformation along with its derivatives with respect to  $\omega$ . The  $\omega$ -domain representation of Eq.(46) is:

$$\Phi_{F_K}(\omega) = \sum_{i=k}^N \sum_{j=\max(\theta, i-r)}^{\min(\theta, N-r)} \binom{N-r}{j} \binom{r}{i-j} (-1)^{i-k-\ell} \frac{\sum_{\theta_0=0}^{N-r-k} \sum_{\theta_1=0}^{N-r-k} \dots \sum_{\theta_{M-1}=0}^{N-r-k} \Psi(N-r-k; \theta_0, \dots, \theta_{M-1})}{\prod_{v=0}^{M-1} [\Gamma(v+1)]^{\theta_v}} \sum_{\theta_2=0}^{r-\ell} \dots \sum_{\theta_M=0}^{r-\ell} \Psi(r-\ell; \theta_1, \dots, \theta_M) \frac{\Gamma\left(\sum_{\gamma=0}^{M-1} \theta_\gamma + 1\right)}{\left(\omega + N - r - k + \sum_{\eta=1}^M \theta_\eta c_\eta\right)^{\sum_{\gamma=0}^{M-1} \theta_\gamma + 1}} \quad (48)$$

Where the definition of the term  $\Psi(S; i_1, i_2, \dots, i_M)$  is as follows:

$$\Psi(S; i_1, i_2, \dots, i_M) \triangleq \begin{cases} \frac{S!}{i_1! i_2! \dots i_M!} & \text{for } S = i_1 + i_2 + \dots + i_M \\ 0 & \text{for } S \neq i_1 + i_2 + \dots + i_M \end{cases} \quad (49)$$

On the other hand, the Laplace transformation of Eq.(51) is analytically very complicated and therefore the numerical techniques is the only way that allows us to compute this transformation.

In order to analyze the processor detection performance in uniform clutter background, the CF of the random variable  $Z_{OS}$  is required. By letting  $r=0$  in Eq.(42), this CF can be expressed as [14]

$$C_{Z_{OS}}(\omega) = \frac{K}{\Gamma(M)} \binom{N}{K} \sum_{i=0}^{K-1} \binom{K-1}{i} (-1)^{K-i-1} \Phi_1(i, \omega) \quad (50)$$

Where

$$\Phi_1(i, \omega) \triangleq \sum_{k_1=0}^{N-i-1} \sum_{k_2=0}^{N-i-1} \dots \sum_{k_{M-1}=0}^{N-i-1} \left\{ \prod_{q=1}^M \left( \frac{1}{\Gamma(k_q + 1) [\Gamma(q)]^{k_q}} \right) \Gamma(N-i) \right\} \frac{\Gamma(\beta)}{(\omega + N - i)^\beta} \quad (51)$$

With

$$\beta \triangleq M + \sum_{\alpha=2}^M (\alpha-1) k_\alpha \quad \& \quad \sum_{j=1}^M k_j = N - i - 1 \quad (52)$$

Since the CF of the noise power level estimate  $Z_{OS}$  represents the backbone of its processor detection performance, the evaluation of this performance

becomes an easy task once that function is obtained. Finally, the  $\ell$ th derivative of this CF is given by:

$$\frac{d^\ell}{d\omega^\ell} \{C_{Z_{OS}}(\omega)\} = \frac{K}{\Gamma(M)} \binom{N}{K} \quad (53)$$

$$\sum_{i=0}^{K-1} \binom{K-1}{i} (-1)^{K-i-1} \frac{d^\ell}{d\omega^\ell} \{\Phi_1(i, \omega)\}$$

With

$$\frac{d^\ell}{d\omega^\ell} \{\Phi_1(i, \omega)\} = \sum_{k_1=0}^{N-i-1} \sum_{k_2=0}^{N-i-1} \dots \sum_{k_{M-1}=0}^{N-i-1} \left\{ \prod_{q=1}^M \left( \frac{1}{\Gamma(k_q + 1) [\Gamma(q)]^{k_q}} \right) \Gamma(N-i) \right\} \frac{(-1)^\ell (\beta)_{\ell}}{(\omega + N - i)^{\beta+\ell}} \quad (54)$$

Again, the OS-CFAR processor performance is highly dependent upon the value of K. For example, if a single extraneous target appears in the reference window of thr appreciable magnitude, it occupies the highest ranked cell with high probability. If K is chosen to be N, the estimate will often set the threshold based on the value of the interfering target. This increases the overall threshold and may lead to a target miss. If, on the other hand, K is chosen to be less than the maximum value, the OS-CFAR scheme will be influenced only slightly for up to N-K spurious targets.

A desirable CFAR scheme would of course be one that is insensitive to changes in the total noise power within the reference window cells so that a constant false alarm rate is maintained. This is actually the case of the two architectures under consideration.

#### 4. Performance Evaluation Results

In this section, we present some representative numerical results, which will give an indication of the tightness of our previous analytical expressions. The performance of CFAR processors for partially-correlated  $\chi^2$  fluctuating targets is numerically evaluated for some parameter values and the results of these evaluations are presented in several sets of figures. The first set includes Figs.(2-3) and concerns with the detection performance of CA and OS schemes, respectively, for a number of integrated pulses of 2, 3, and 4 along with the single-sweep case which is included as a reference for comparison, when the radar target fluctuates in accordance with partially-correlated  $\chi^2$  model with two and four degrees of freedom.

Since the performance of OS processor is strongly dependent on the ranking order parameter K, we choose the value that corresponds to the optimum detection performance in uniform noise background which is 21 for N=24 [8]. The displayed results of these figures show that for low values of SNR, the fully-correlated case ( $\rho_r=1.0$ ) gives higher detection performance than the fully de-correlated ( $\rho_r=0$ ) case. As the target return becomes stronger, an alternative version of the above behavior is observed, where the non-correlated performance surpasses the fully-correlated one. It is also noted that for M=2, the processor detection



performance for  $\rho_1 = 1$  &  $\rho_1 = 0$  coincides with its detection performance for  $\rho_1 = 2$  &  $\rho_1 = 1.0$ . In addition, the non-correlated and fully-correlated detection performances embrace all the partially-correlated cases in either situation.

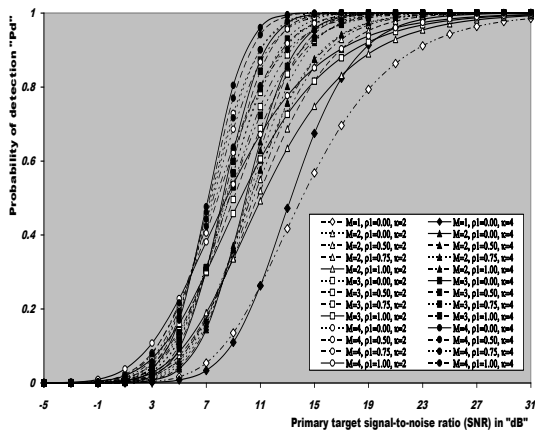


**Fig. 2.** M sweeps ideal detection performance of CA scheme for partially correlated  $\pi^2$  targets with 2&4 degrees of freedom when  $N=24$ , and  $Pfa= 1.0E-6$

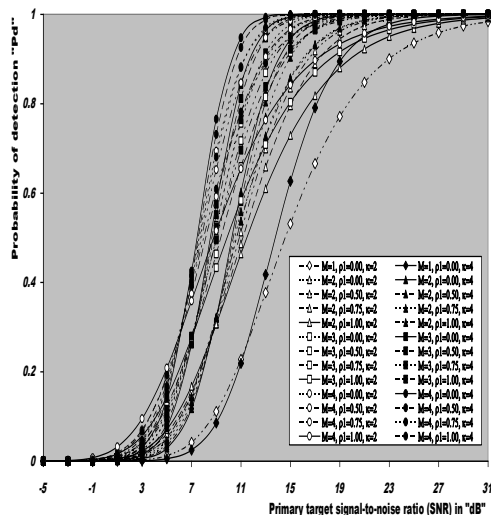


**Fig. 3.** M sw sweeps ideal detection performance of Os(21) scheme for partially correlated  $\pi^2$  targets with 2&4 degrees of freedom when  $N=24$ , and  $Pfa= 1.0E-6$

This observation is common for any number of integrated pulses. Additionally, the partially-correlated  $\chi^2$  with  $\rho_1 = 2$  offers higher detection performance than that of  $\rho_1 = 1$  when the target return becomes stronger while the reverse of this behavior occurs when the target return is modest. Moreover, as  $M$  increases, the processor detection performance ameliorates and the reversing point is shifted towards lower values of SNR. By reversing point, we mean the point at which the detection performance changes its superiority from

fully-correlated to fully-uncorrelated. All the presented results are obtained for a constant false alarm rate of  $10^{-6}$  and a reference window of size 24 cells.

To make a comparison between the performances of the underlined CFAR schemes and that of the optimum detector, the second group of illustrations includes Figs.(4-7). This category contains the partially-correlated  $\chi^2$  target homogeneous detection performance of the CA and OS schemes along with the optimum processor for  $M=2$  and 4. The curves of this set are labeled in the CFAR procedure and the correlation coefficient ' $\rho_1$ ', respectively. The indication OT, A, or O on a specified curve means that it is drawn for optimum, cell-averaging, or order-statistic detector, respectively. It is important to note that Figs.(4-5) describe the performance of the three processors when the primary target fluctuates following partially-correlated  $\chi^2$  model with two and four degrees of freedom, respectively, for  $M=2$ , while Figs.(6-7) depict the same thing for  $M=4$ . In any situation, it is noticed that the performance of CA algorithm is the much closer one to that of the optimum detector under any operating conditions and the OS scheme comes next. All the indicated remarks on the results of Figs.(2-3) are clearly demonstrated on the results of the present figures. For weak SNR, the processor performance degrades as  $\rho_1$  decreases, while for strong SNR this performance improves as  $\rho_1$  decreases. This observation is noticed for partially-correlated  $\chi^2$  targets fluctuating with either two or four degrees of freedom. In addition, these plots illustrate the superiority of  $\chi^2$  fluctuation model with four degrees of freedom over that following  $\chi^2$  model with two degrees of freedom, especially for large SNR. As the number of non-coherent integrated pulses increases, the processor performance improves and less SNR value is needed to achieve the same level of detection.

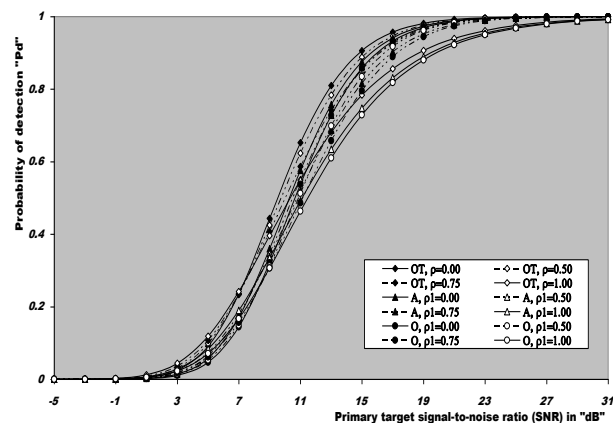


**Fig. 4.** M-sweep ideal detection performance of CFAR processor for partially- correlated  $\pi^2$  targets with two degrees of freedom when  $N=24$ ,  $M=2$ ,  $Pfa=1.0E-6$

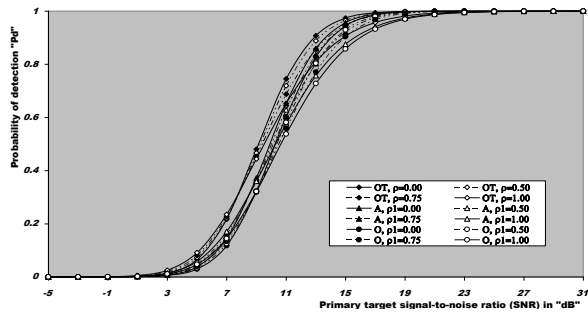


Fig. 5. M sweep ideal detection performance of CFAR processor for partially- correlated  $\pi^2$  targets with two degrees of freedom when  $N=24$ ,  $M=2$ ,  $Pfa=1.0E-6$

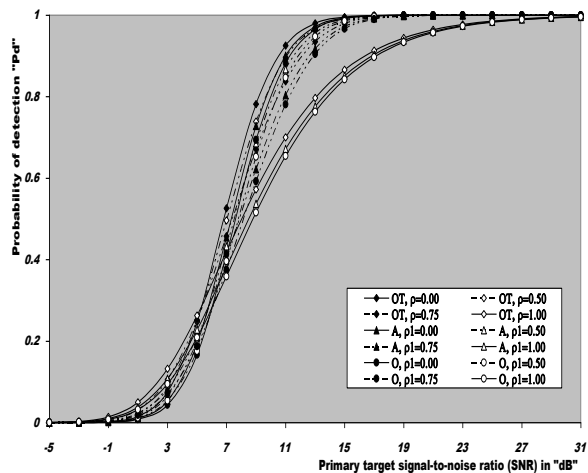


Fig. 6. M-sweep ideal detection performance of CFAR processor for partially- correlated  $\pi^2$  targets with two degrees of freedom when  $N=24$ ,  $M=4$ ,  $Pfa=1.0E-6$

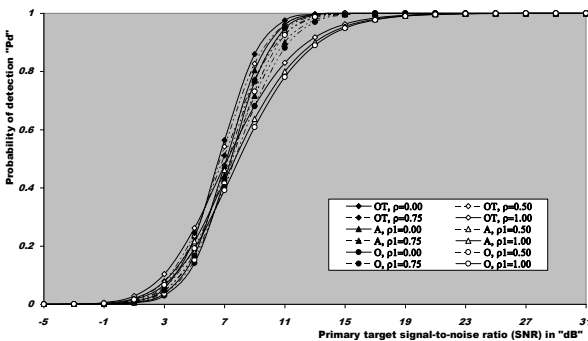


Fig. 7. M-sweep ideal detection performance of CFAR processor for partially- correlated  $\pi^2$  targets with four degrees of freedom when  $N=24$ ,  $M=4$ ,  $Pfa=1.0E-6$

In the next group of figures, we are concerned with what is known, in the world of the radar target detection, as receiver operating characteristics (ROC's). These characteristics describe the detection probability as a function of the false alarm probability for a fixed target signal strength ( $SNR=const$ ). This set of figures incorporates Figs.(8-9) which represent the ROC's of CA and OS(21), respectively. In these figures, the

processor detection performance is plotted against the false alarm rate for a number of integrated pulses of 2 and 4 when the primary target fluctuates in accordance with  $\chi^2$  distribution with two and four degrees of freedom. Since the fully correlated and fully de-correlated cases enclose the partially-correlated situations, we restrict our evaluations to these two border limits ( $\rho_1=0$  &  $\rho_1=1$ ). The reference window size is taken as 24 and the primary target signal strength is taken as 5dB. For comparison, the single sweep ROC's is also included in these plots.

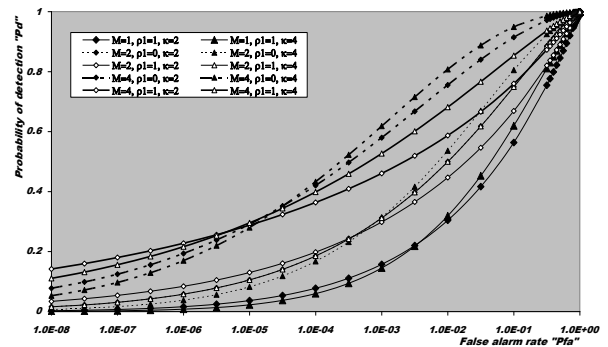


Fig. 8. M-sweeps receiver operation characteristics (ROC's) of CA processor for partially – correlated  $\pi^2$  targets in homogeneous situation when  $N=24$  and 5db

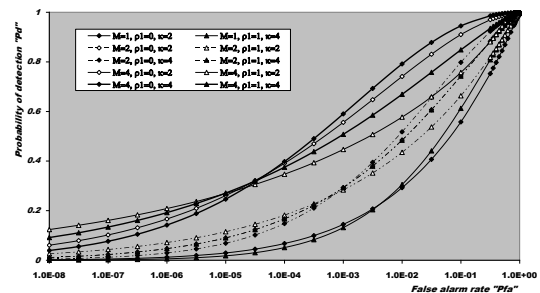
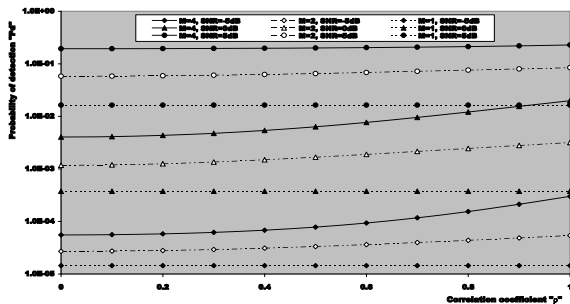


Fig. 9. M-sweeps receiver operation characteristics (ROC's) of Os (21)scheme for partially – correlated  $\pi^2$  targets when  $N=24$ , and  $\Omega=5db$

The curves of these figures are labeled in the number of the post-detection integrated pulses and the correlation coefficient of the primary target returns ( $\rho_1$ ). The displayed results show that for lower false alarm rates, the processor detection probability improves as  $\rho_1$  increases. As the false alarm rate increases, this behavior is rapidly reversed and the fully de-correlated detection performance surpasses that corresponding to the fully correlated case. Additionally, as the number of non-coherent integrated pulses increases, the reversing point or the critical rate, moves towards the lower false alarm rate and this is common either the target fluctuates following  $\chi^2$  with two or four

degrees of freedom. Moreover, the processor detection performance for  $\chi^2$  distribution with  $\square = 2$  is superior to that for  $\chi^2$  distribution with  $\square = 1$  in the case where the operating false alarm rate is higher than its critical value. If the operating false alarm rate is lower than its critical rate, the processor detection performance when the fluctuation of the primary target follows  $\chi^2$  distribution with  $\square = 1$  surpasses its performance when this fluctuation obeys  $\chi^2$  distribution with  $\square = 2$ . No forget that when  $M=2$ , the processor ROC's for  $\square = 1$  &  $\square_1=0$  coincide with its ROC's for  $\square = 2$  &  $\square_1=1$ . The results of this group confirm the observed remarks on the previous groups as well as demonstrate our comments on the behavior of their figures. Additionally, the homogeneous detection performance of CA scheme is always superior to that of OS algorithm, under the same operating conditions, as predicted.

To illustrate the influence of the signal correlation on the processor detection performance, the next group is devoted to the processor detection performance against the correlation coefficient between the radar target returns given that the number of integrated pulses ( $M$ ) as well as the signal strength (SNR) is held constant. Figs (10-11) distinctly show these characteristics for the underlined detectors, CA and OS(21), respectively, for SNR=-5, 0, and 5dB when  $M=1, 2$ , and 4, given that the radar target fluctuates in accordance with  $\chi^2$  distribution with  $\square = 1$ . Since the chosen signal strength is modest, the scheme detection performance improves as the target returns become highly correlated.



**Fig. 10.** M sweeps variation of ideal detection performance CA-CFAR processor for partially correlated Rayleigh fluctuating targets when  $N=24$ ,  $P_{fa}=1.0E-6$  and  $SNR= -5,0 \& 5dB$

This result is predicted since the correlation strengthens the weak signal returns in contrast to the case in which the signal returns are strengthened where the correlation weakens the signal returns. For the same reason, the rate of improvement decreases as the number of the consecutive sweeps increases. Moreover, this rate of improvement increases as the target signal returns

become weaker, given that the number of integrated pulses is maintained constant.

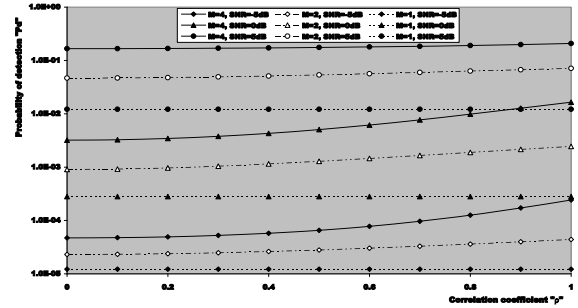


**Fig. 11.** M sweeps variation of the ideal detection performance OS(21)-CFAR processor for partially correlated Rayleigh fluctuating targets when  $N=24$ ,  $P_{fa}=1.0E-6$  and  $SNR= -5,0 \& 5dB$

The two processors under consideration give approximately the same level of detection for correlated signal returns without any superiority between them. This concluded remark is also predicted due to the fact that the CFAR schemes behave likely for modest target signal strength, as the above mentioned results demonstrate. Finally, if the primary target fluctuates in accordance with  $\chi^2$  distribution with  $\square = 2$ , the underlined processors act the same behavior with minor improvement in each case.

Now, let us turn our attention to the processor performance when the operating environment is contaminated with several spurious targets along with the underlined primary target. In other words, our concern here is to show the impact of non-homogeneous operating environment on the detection of partially-correlated targets by adaptive processors. To attain this request, we provide a variety of numerical results for the performance of CA- and OS-CFAR processors in the multiple target situations. Since the optimum value of  $K$ , for a reference window of size 24, is 21, we have assumed that there are three interfering target returns amongst the contents of the estimation cells. The motivation for this assumption is to calculate the highest detection performance of OS scheme in multi-target environment. This value of extraneous target returns is the maximum allowable value before the OS performance degradation occurs. Our numerical results are obtained for a possible practical situation where the primary and the secondary interfering targets fluctuate in accordance with the  $\chi^2$  fluctuation model with the same correlation coefficient ( $\rho_1=\rho_2=\square$ ), and of the equal target return strength ( $INR=SNR$ ). Additionally, for our new results to be comparable with the older ones (in the absence of outlying targets), the design rate of false alarm is held unchanged ( $P_{fa}=10^{-6}$ ).

The obtained results are classified to categories. The first category, including Figs.(12 & 13), depicts the detection performance of the CA and OS(21) schemes, respectively, under the same operating conditions as in Figs.(2 & 3) with the exception that three spurious targets are allowed to be present amongst the candidates of the reference set.

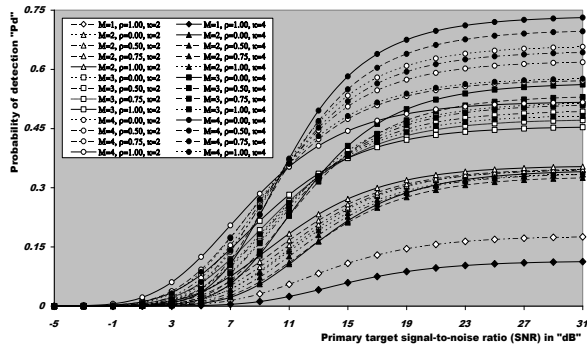


**Fig. 12.** Multitarget detection performance of CA scheme for partially correlated  $\pi^2$  targets with 2&4 degrees of freedom when  $N=24$ ,  $r=3$ , and  $P_{fa}= 1.0E-6$

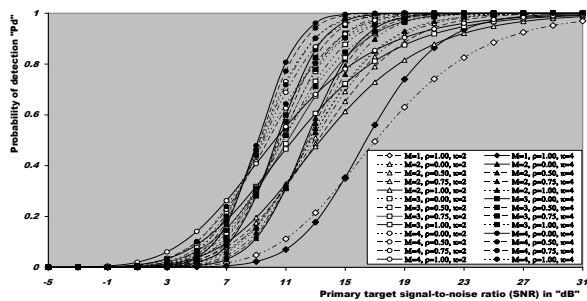


**Fig. 13.** Multitarget detection performance of OS(21) scheme for partially correlated  $\pi^2$  targets with 2&4 degrees of freedom when  $N=24$ ,  $r=3$ , and  $P_{fa}= 1.0E-6$

The curves of these figures are labeled in the number of integrated pulses ( $M$ ), the strength of the correlation between the target returns ( $\square$ ) and the parameter that represents the degrees of freedom ( $\square$ ). For comparison, the single sweep case is included in these plots. In addition to the partially-correlated cases, the well-known four Swerling's models are also included. It is important to note that the full scale of the  $P_d$  axis in this case of CA scheme has a maximum value of 75%. There is another interesting point about the reaction of CFAR schemes against  $\chi^2$  fluctuation model where the SWII & SWIII performances are coincide for  $M=2$ . The displayed results show that the behavior of the CFAR processors in the presence of extraneous targets is similar to that of in their absence. By comparing the results of Fig.(12) to the corresponding ones of Fig.(13), we observe that intolerable masking of the primary target occurs in the case of CA procedure and the OS(21) architecture is capable of resolving

multiple targets in the reference window as long as their number is within its allowable values ( $r \leq N-K$ ). All the concluded remarks about the ideal performance of CA and OS(21) schemes are also observed on their multi-target performance given that the target under test along with the interfering ones fluctuate obeying  $\chi^2$  model with 2 and 4 degrees of freedom.

As the displayed results of Figs (12 & 13) demonstrate, it is obvious that the CA procedure is unable to resolve the problem of detecting the partially-correlated targets in the presence of the outlying targets. Therefore, we will go to show the effects of choosing parameters on the behavior of the OS algorithm against the detection of this important class of fluctuating targets. It is well-known that the OS technique gives good multi-target performance as the number of spurious targets doesn't exceed its upper limit which is ( $r \leq N-K$ ). To verify this condition, Fig (14) illustrates the multi-target detection performance of OS(21) when the operating environment contains 3, 5, and 10 interferers along with the target under investigation.

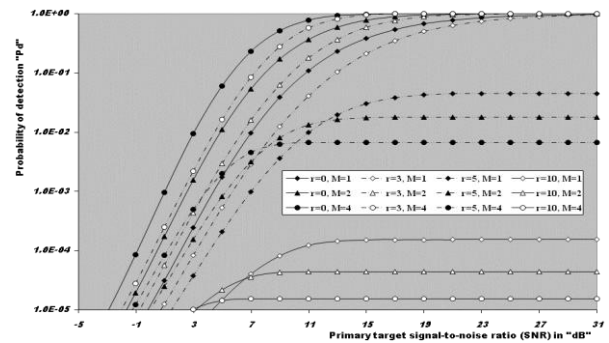


**Fig.14.** M- sweep multi target detection performance of OS(21) processor for partially- correlated  $\pi^2$  targets with two degrees of freedom when  $N=24$ ,  $INR=SNR$ ,  $p=0$  and  $P_{fa}=1.0E-6$

The primary and the secondary interfering targets are assumed to be fluctuating following  $\chi^2$ -distribution with two degrees of freedom and with a null correlation coefficient ( $\rho=0$ ). As a reference of comparison, the ideal detection performance ( $r=0$ ) of the underlined scheme is also included in this figure. Additionally, the displayed results are obtained on the assumption that the extraneous target gives a signal of the same strength as that given by the primary target ( $INR=SNR$ ). Moreover, the processor is assumed to collect data from two or four consecutive sweeps ( $M=2$  or 4) in order to take its decision. The mono-pulse detection performance is incorporated amongst the contents of the underlined figure to show to what extent the post-detection integration can improve the performance of the CFAR technique. Since the detection probability for  $r>N-K$  is very weak, we draw the obtained results on a logarithmic scale in order to be able to illustrate weak

as well as the strong values. The family curves of this figure shows that the OS (21) presents good performance in the absence ( $r=0$ ) as well as in the presence of outlying targets given that their number is less than or equal 3. If this condition is failed, a noticeable degradation in the processor performance is observed. The rate of degradation increases as the number of interferers becomes more and more. In this situation, it is obvious that there is an improvement in the processor performance as  $M$  increases for low SNR. For strong signal return, on the other hand, the processor performance degrades as  $M$  increases. This behavior of the OS (21) against the presence of the spurious targets in the operating environment is predicted since the density of these targets exceed their allowable range. For example if  $r=5$  and  $K=21$ , then three of them are eliminated and the rest incorporate in constructing the detection threshold. This in turn pushes the detection threshold towards its higher values and consequently the detection probability goes towards its weaker values. As the number of the integrated pulses increases, the interfering target return becomes stronger and the detection threshold attains higher values and this leads to make the detection probability weaker and weaker. For this reason the processor performance degrades as the number of non-coherent integrated pulses increases given that  $r > N-K$ . This degradation becomes worst as the reference window becomes full of extraneous targets as the displayed results demonstrate. This behavior of the OS algorithm against the presence of partially-correlated  $\chi^2$  target returns amongst the candidates of the reference set when these returns are de-correlated ( $\rho=0$ ) which means that these targets fluctuate in accordance with SWII model. Fig.(15) depicts the same thing as Fig.(14) except that the fluctuation of the primary as well as the secondary outlying targets follows  $\chi^2$  statistics with two degrees of freedom when the target returns are fully-correlated ( $\rho=1.0$ ) which indicates that they obey SWI mode in their fluctuation.

In contrast to the behavior against SWII fluctuating targets, the OS performance improves as  $M$  increases irrespective to the strength of the target return either weak or strong. This reaction of the OS scheme against SWI fluctuating targets is waited since the correlation between the target returns weakens its associated power. In addition, the rate of degradation, as  $r$  increases, is less than in the case of SWII targets. Moreover, the rate of improvement, as the number of the non-coherent integrated pulses increases, is clearer than in the situation where the target fluctuation follows SWII model.

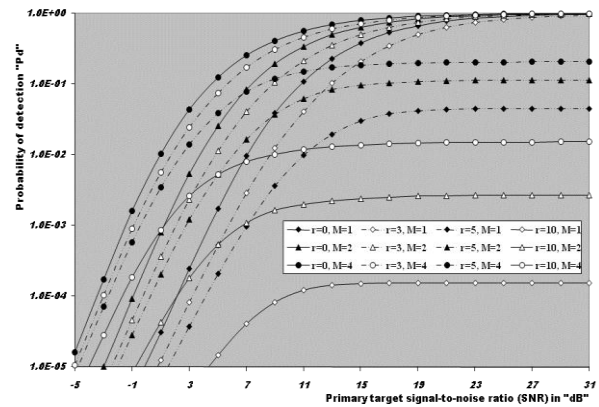
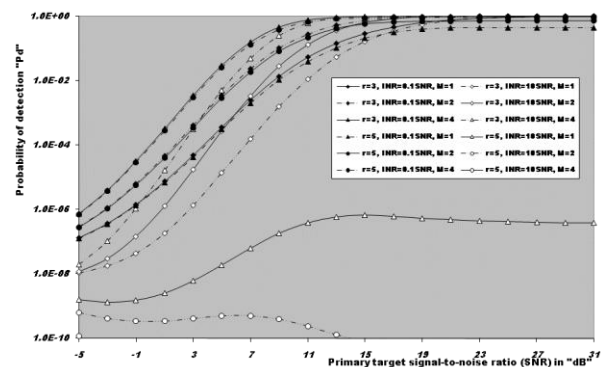


Fig.(15) M-sweeps multitarget detection performance of OS(21) processor for partially-correlated  $\pi^2$  targets with two degrees of freedom when  $N=24$ ,  $INR=SNR$ ,  $\rho=1.0$ , and  $Pfa=1.0E-6$ .

**Fig. 15.** M- sweep multi target detection performance of OS(21) processor for partially- correlated  $\pi^2$  targets with two degrees of freedom when  $N=24$ ,  $INR=SNR$ ,  $p=1.0$  and  $Pfa=1.0E-6$

In the next category of curves, we turn our attention to the impact that the strength of the outlying target return may affect the detection of the partially-correlated  $\chi^2$  targets. This category, including Figs.(16-17), illustrates the multi-target detection performance of OS(21) processor in the case where the principal and the spurious targets fluctuate following  $\chi^2$  model with 4 degrees of freedom when  $\rho$  equals zero and one, respectively. In each one of these situations, we evaluate the detection performance for weak, relative to the primary target returns, interfering target returns ( $INR=SNR/10$ ) as well as strong level of interference ( $INR=10SNR$ ) when the OS (21) scheme builds its decision on single, double, and four consecutive sweeps given that the operating environment is contaminated with three or five spurious targets. The displayed results demonstrate that the presence of the outlying targets has little effect on the processor performance when the strength of their returns is weak.



**Fig. 16.** M- sweep multi target detection performance of OS(21) scheme for partially- correlated  $\pi^2$  targets with four degrees of freedom when  $N=24$ ,  $p=.0$  and  $Pfa=1.0E-6$

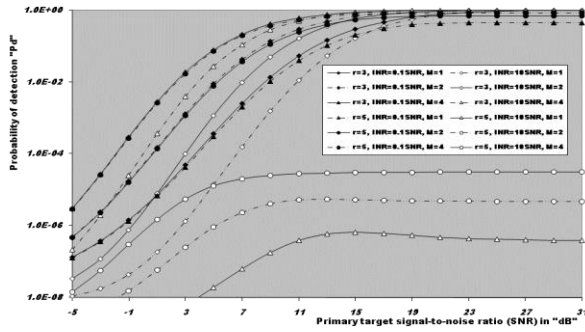


**Fig.17.** M- sweep multi target detection performance of OS (21) scheme for partially- correlated  $\pi^2$  targets with four degrees of freedom when  $N=24$ ,  $p=1.0$  and  $Pfa=1.0E-6$

When these returns become stronger, they severely degrade the reaction of the OS scheme against the presence of the secondary target returns amongst the reference samples especially if their numbers surpass the allowable range. However, if the interfering returns are weak, the OS processor maintains its immunity to the presence of the outlying targets even though their number exceeds the allowable range as Fig.(16) demonstrates. This result is predicted since the weak returns resemble the background samples and have negligible effect on the changing of the detection threshold. It is of importance to note that the  $K^{\text{th}}$  reference sample is the only one that is responsible for building the threshold in OS (K) scheme. This means that the presence of the interferers has no effect on the detection threshold given that their returns are comparable to the content of the reference noise samples. Additionally, the displayed results confirm the more degraded detection performance as the number of the post-detection integrated pulses increases, even though their number is within the allowable range, if the interferer's returns are stronger than the primary target return. On the other hand, if the interfering target returns are strong and their number exceeds the allowable range, the OS performance becomes worst. Fig.(16) describes the OS behavior against interfering targets when the primary as well as the spurious targets fluctuate following SWIV model, whilst Fig.(17) depicts the OS multi-target performance in the case where the tested target along with the secondary outlying ones fluctuate in accordance with SWIII model. The differences between Figs (16 & 17) are approximately similar to those between Figs.(14 & 15). Finally, the variations of the false alarm rate with the strength of the interfering target returns are plotted, in the last category of curves, for the underlined architectures when reacted to  $\chi^2$  fluctuating targets with 2 and 4 degrees of freedom. This set of figures includes Figs (18-19).

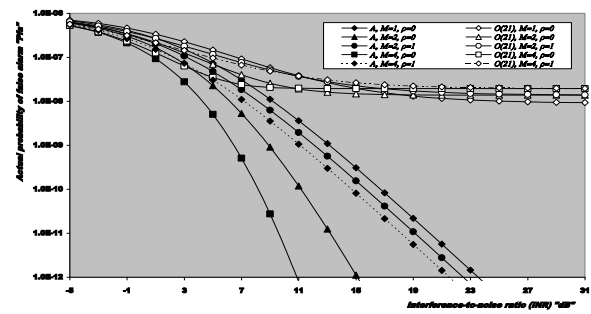


**Fig. 18.** M-sweeps false alarm rate performance as a function of the interfering target strength (INR) of the CFAR schemes for  $\pi^2$  fluctuating targets when  $N=24$ ,  $r=3$  and design  $Pfa=1.0E-6$

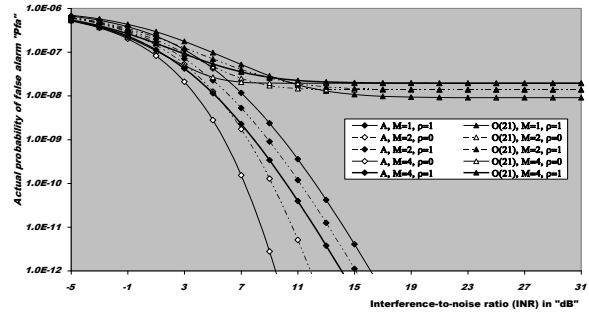


**Fig. 19.** M-sweeps false alarm rate performance as a function of the interfering target strength (INR) of the CFAR schemes for  $\pi^2$  fluctuating targets when  $N=24$ ,  $r=3$  and design  $Pfa=1.0E-6$

In this case, the primary and the secondary outlying targets are assumed to be fluctuating with the same degree of freedom and our numerical results are constrained to the two limits of the correlation coefficient ( $\rho=0$ ,  $\rho=1$ ) which are corresponding to the well-known Swerling's models. The curves of these figures are labeled in the specified processor (A: for cell-Averaging, O: for Order-statistic), the number of the integrated pulses  $M$  and the Swerling fluctuation model. The numerical results of these figures are given for a design rate of false alarm of  $10^{-6}$  and a reference window of the size 24 samples. The interfering targets are assumed to exhibit  $\chi^2$  statistics with full correlation ( $\rho=1$ ), which corresponds to SWI, when the degree of freedom is 2, or SWIII, when the degree of freedom is 4. On the other hand, when the outlying targets exhibit  $\chi^2$  statistics with null correlation ( $\rho=0$ ), the resulting fluctuation model is SWII, in the case where the degree of freedom is 2, or SWIV, in the case where the degree of freedom is 4. The results of these figures show that the false alarm rate performance of the CA processor degrades as the strength of the interfering target return (INR) increases, and the rate of degradation decreases as  $\rho$  increases or the degree of freedom decreases. This statement is common for the CFAR processors

considered here. However, the OS(21) scheme has the lowest rate of degradation and consequently it is the only processor that is capable of maintaining the false alarm rate at approximately the desired value, given that the number of spurious target returns doesn't exceed its allowable values. In addition, when the INR becomes very high, the behavior of the OS detector is independent on the correlation coefficient  $\rho$  and tends to be constant. Moreover, the OS false alarm rate performance improves as the number of post-detection integrated pulses increases, which is not offered by the CA technique. This result is expected since the largest interfering target returns occupy the top ranked cells and therefore they are not incorporated in the estimation of the background noise power level. In other words, the noise estimate is free of extraneous target returns and therefore it represents the homogeneous background environment. Consequently, the false alarm rate performance of the OS procedure improves as the number of non-coherent integrated pulses increase.

## 5. Conclusion

This paper addresses the detection probability of a radar receiver which the post-detection integrates  $M$  pulses of an exponentially correlated signal from a Rayleigh target in thermal noise is calculated. At the limiting correlation coefficients,  $\rho=1$  and  $\rho=0$ , the analysis yields, respectively, the well-known SWI and SWII models. In addition, the detection probability of the sum of the  $M$  square-law detected pulses is computed for the case where the signal fluctuation obeys  $\chi^2$  statistics with four degrees of freedom. SWIII and SWIV cases represent the situations where the signal is completely correlated and completely de-correlated, respectively, from pulse to pulse. Moreover, we have analyzed the performance of CFAR processors for partial signal correlation in these two situations. These processors include the well-known candidates in the world of CFAR: CA and OS schemes. CA has the best homogeneous performance while the OS has its immunity to the presence of the outlying targets as long as their number lies within the allowable range. We have derived the exact false alarm and detection probabilities, in the absence as well as in the presence of extraneous targets, for the condition of partial signal correlation. The primary and the secondary interfering targets are assumed to be fluctuating in accordance with  $\chi^2$ -distribution with two and four degrees of freedom. The analytical results have been used to develop a complete set of performance curves including ROC's, detection probability in homogeneous and multi-target situations, required SNR to achieve a prescribed values of  $P_{fa}$  &  $P_d$ , and the variation of the false alarm rate

with the strength of the interfering target returns that may exist amongst the contents of the estimation set. As expected, the detection performance of the CFAR detectors for partially-correlated  $\chi^2$  targets with two degrees of freedom is between that for SWI and SWII models, while it lies between those of SWIII and SWIV models in the case where the targets obey, in their fluctuation,  $\chi^2$  statistics with four degrees of freedom. In any one of these fluctuating families, more per pulse signal-to-noise ratio is required to achieve a prescribed probability of detection as the signal correlation increases from zero to unity. In addition, the false alarm rate increases with the signal correlation and the OS architecture is the only, relative to the CA scheme, processor that is capable of maintaining a constant rate of false alarm, irrespective to the interference level, in the case where the spurious target returns occupy the top ranked cells and they are within their allowable values. As a final conclusion, the detection performance of a CFAR procedure is related to the target model, the number of post-detection integrated pulses, and the average power of the target.

The results for partial-correlation fall between those for the two extremes of complete de-correlation and complete correlation. Thus, to estimate the performance for partially-correlated pulses, interpolation between the results for completely correlated and completely de-correlated conditions can be used as an approximation.

When the target signal fluctuates obeying  $\chi^2$  statistics, the signal components are correlated from pulse to pulse and this correlation degrades the processor performance. A common and accepted practice in radar system design to mitigate the effect of the target fluctuation is to provide the frequency diversity to de-correlate the signal from pulse to pulse. While this technique is effective, it requires additional system complexity and cost

## REFERENCES

- [1] Meyer. D. P and Meyer. H. A, "**Radar target detection**", *Academic Press, INC.* 1973.
- [2] Hou. X. Y, Morinaga. N and Namekawa. T, "**Direct evaluation of radar detection probabilities**", *IEEE Transactions on Aerospace and Electronic Systems*, AES-23, No.4, pp. 418-423, Jul 1987.
- [3] Weiner. M. A, "**Detection probability for partially correlated chi-square targets**", *IEEE Transactions on Aerospace and Electronic Systems*, AES-24, No.4, pp. 411-416, July 1988.
- [4] El Mashade, M. B, "**M-sweeps detection analysis of cell-averaging CFAR processors in multiple target situations**", *IEE Proc.-Radar*,

- Sonar Navig.*, Vol.141, No.2, pp. 103-108, April 1994.
- [5] Aloisio. V., di Vito, A and Galati. G, **“Optimum detection of moderately fluctuating radar targets”**,*IEE Proc.-Radar, Sonar Navig.*, Vol.141, No.3, pp. 164-170, June 1994.
- [6] Swerling.P, **“Radar probability of detection for some additional fluctuating target cases”**, *IEEE Transactions on Aerospace and Electronic Systems, AES-33*, pp. 698-709, April 1997.
- [7] di Vito. A and Nadli, M, **“Robustness of the likelihood ratio detector for moderately fluctuating radar targets”**, *IEE Proc.-Radar, Sonar Navig.*, Vol.146, No.2, pp. 107-112, April 1999.
- [8] El Mashade. M. B, **“Postdetection integration analysis of the excision CFAR radar target detection technique in homogeneous and nonhomogeneous environments”**, *Signal Processing (ELSEVIER)*, Vol.81, pp. 2267-2284, 2001.
- [9] El Mashade. M. B, **“Performance Comparison of a Linearly Combined Ordered-Statistic Detectors under Postdetection Integration and Nonhomogeneous Situations”**,*Journal of Electronics (China)*, Vol.23, No.5pp. 698-707, ,September 2006.
- [10] El Mashade. M. B, **“Analysis of CFAR detection of fluctuating targets”**, *Progress in Electromagnetics Research C*, Vol.2, pp.127-158, 2008.
- [11] El Mashade. M. B, **“Performance analysis of OS structure of CFAR detectors in fluctuating target environments”**, *Progress in Electromagnetics Research C*, Vol.2, pp.127-158, 2008.
- [12] El Mashade. M. B, **“M-correlated sweeps performance analysis of adaptive detection of radar targets in interference-saturated environments”**,*Ann. Telecomm*, Vol.66, pp.617-634, 2011.
- [13] El Mashade. M. B, **“Analytical performance evaluation of optimum detection of  $\chi^2$  fluctuating targets with M-integrated pulses”**, *Electrical and Electronic Engineering*, Vol 1, No 2, pp. 93-111, 2011.
- [14] El Mashade. M. B, **“Anaysis of adaptive detection of moderately fluctuating radar targets in target multiplicity environments”**, *Journal of Franklin Institute*, Vol.348, pp.941-972, 20011.
- [15] El Mashade, M. B, **“Performance Analysis of CFAR Detection of Fluctuating Radar Targets in Nonideal Operating Environments”**, *International Journal of Aerospace Sciences* 2012, Vol.1, No. (3), pp. 21-35, 2012.